Inorganic Chemistry

Article

pubs.acs.org/IC

Trifunctional Metal Ion-Catalyzed Solvolysis: Cu(II)-Promoted Methanolysis of *N*,*N*-bis(2-picolyl) Benzamides Involves Unusual Lewis Acid Activation of Substrate, Delivery of Coordinated Nucleophile, Powerful Assistance of the Leaving Group Departure

Mark A. R. Raycroft, Christopher I. Maxwell, Robyn A. A. Oldham, Areen Saffouri Andrea, Alexei A. Neverov, and R. Stan Brown*

Department of Chemistry, Queen's University, Kingston, Ontario, Canada K7L 3N6

Supporting Information

ABSTRACT: The methanolyses of Cu(II) complexes of a series of *N*,*N*-bis(2-picolyl) benzamides (**4a**−**g**) bearing substituents X on the aromatic ring were studied under $^{s}_{s}$pH-controlled conditions at 25 °C. The active form of the complexes at neutral $^{s}_{s}$pH has a stoichiometry of **4**:Cu(II):($^{-}$OCH$_3$)(HOCH$_3$) and decomposes unimolecularly with a rate constant k_x. A Hammett plot of log(k_x) vs σ_x values has a ρ_x of 0.80 ± 0.05. Solvent deuterium kinetic isotope effects of 1.12 and 1.20 were determined for decomposition of the 4-nitro and 4-methoxy derivatives, **4b**:Cu(II):($^{-}$OCH$_3$)(HOCH$_3$) and **4g**:Cu(II):($^{-}$OCH$_3$)(HOCH$_3$), in the plateau region of the $^{s}_{s}$pH/log(k_x) profiles in both CH$_3$OH and CH$_3$OD. Activation parameters for decomposition of these complexes are $\Delta H^{\ddagger}$ = 19.1 and 21.3 kcal mol^{-1} respectively and $\Delta S^{\ddagger}$ = −5.1 and −2 cal K^{-1} mol^{-1}. Density functional theory (DFT) calculations for the reactions of the Cu(II):($^{-}$OCH$_3$)(HOCH$_3$) complexes of **4a,b** and **g** (**4a**, X = 3,5-dinitro) were conducted to probe the relative transition state energies and geometries of the different states. The experimental and computational data support a mechanism where the metal ion is coordinated to the *N*,*N*-bis(2-picolyl) amide unit and positioned so that it permits delivery of a coordinated Cu(II):($^{-}$OCH$_3$) nucleophile to the C═O in the rate-limiting transition state (TS) of the reaction. This proceeds to a tetrahedral intermediate ***INT***, occupying a shallow minimum on the free energy surface with the Cu(II) coordinated to both the methoxide and the amidic N. Breakdown of ***INT*** is a virtually barrierless process, involving a Cu(II)-assisted departure of the bis(2-picolyl)amide anion. The analysis of the data points to a trifunctional role for the metal ion in the solvolysis mechanism where it activates intramolecular nucleophilic attack on the C═O group by coordination to an amidic N in the first step of the reaction and subsequently assists leaving group departure in the second step. The catalysis is very large; compared with the second order rate constant for methoxide attack on **4b**, the computed reaction of CH$_3$O^{-} and **4b**:Cu(II):(HOCH$_3$)$_2$ is accelerated by roughly 2.0 × 10^{16} times.

1. INTRODUCTION

The usual ways that metal ions promote solvolytic reactions of carboxylate esters and amides, as well as neutral and anionic organophosphorus esters comprise the following: (1) electrophilic Lewis acid activation of the substrate through X=O or X=S coordination, where X = C or P; (2) intramolecular delivery of metal-coordinated lyoxide nucleophiles; (3) electrostatic stabilization of the transforming substrate-nucleophile species; and (4) electrophilic assistance of the departure of the leaving group (LGA).[1−4] The first three of these roles have been demonstrated with several types of substrates, and particularly for the decomposition of poorly reactive anionic phosphate mono- and diesters or neutral phosphate triesters as well as carboxylate esters and amides. In most of these cases, metal binding ligands are attached to the substrate to position the metal ion close to the X=O or X=S unit to optimize Lewis acid activation. Metal ion catalysis for the decomposition of amides, particularly peptides in metallo-peptidase enzymatic systems, is also of general importance,[5] but less well-described are small molecule systems for the cleavage of carboxamides[6] where the leaving group is not activated. These are notoriously inert to solvolysis of the >N−C═O because of the inherent resonance stability which shields the substrate from nucleophilic attack, and also because of poor leaving group ability of the amide anion from the subsequently formed tetrahedral intermediates.[7] Because the interaction of neutral amides and positively charged metal ions or their complexes in solution, particularly water, is weak, catalyzed solvolysis is depressed further[6e] unless the substrate possesses some mode of attraction such as a pronounced soft-soft interaction,[8] a residue acting as an attractive site,[9] or attached ligands[6b] that positions the metal ion close to the scissile bond. Even so, amides with normal amine leaving groups are generally not very active because of the reluctance of their departure from the tetrahedral intermediate unless they have a low pK_a (e.g.,

Received: July 5, 2012
Published: September 12, 2012

   dx.doi.org/10.1021/ic301454y | *Inorg. Chem.* 2012, 51, 10325−10333

imidazole or anilide) or there is a physical effect such as release of strain (as in distorted amides[10] and lactams[11]).

Recently we communicated a mechanistic study[12] of an unusual methanolysis reaction of the Cu(II)-complex of *N,N*-bis(2-picolyl) acetamide, **1**, the products of which are methyl acetate and Cu(II):*N,N*-bis(2-picolyl)amine. This reaction was the subject of an early report by Houghton and Puttner[13] some 40 years ago describing the methanolysis of some N-acyl derivatives of *N,N*-bis(2-picolyl) amine in the presence of Cu(II). Subsequent physical studies with such amides,[14−16] the demonstration of their synthetic utility[17] as well as the recent reports on the methanolysis of metal complexes of secondary amides[18] and demonstration of mild methanolytic cleavage of a special class of amides, **2**,[19] prompted us to expand a program[20] investigating the scope and importance of metal ion-promoted leaving group assistance (LGA) during the alcoholysis reactions.

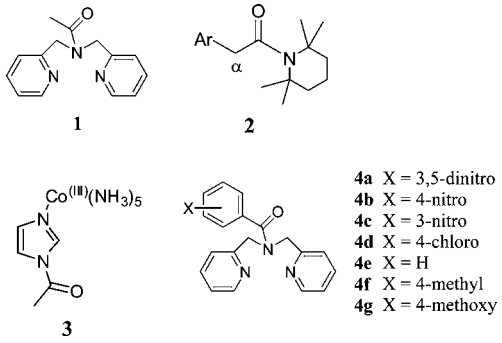

Our initial observation[6e] of where this effect might be operative was during the methoxide reaction of the $(H_3N)_5$Co(III)-complex of acetyl imidazole (**3**); there the second order rate constant for methoxide attack (k_{MeO^-} = 4.69 × 10^7 M^{-1} s^{-1}) was 4 orders of magnitude higher than that for acetyl imidazole itself (k_{MeO^-} = 7.9 × 10^3 M^{-1} s^{-1}). The large acceleration was surmised to result in part from $(H_3N)_5$Co(III)-activation of the acyl group by reducing the imidazole's resonance donation, in part from a methanolic medium induced electrostatic enhancement of the reaction of oppositely charged substrate and nucleophile and partly from the reduction in pK_a of the conjugate acid of the leaving group (10 for H-Im-Co(III)$(NH_3)_5$ vs 14 for H-Im)[21] as a consequence of LGA. In the case of **1**:Cu(II), the metal ion enacted a trifunctional role[12] (which we term as trifunctional catalysis) to accelerate the methanolysis by (1) positioning the metal ion close to the amide N, binding to its lone pair to reduce amidic resonance; (2) binding and intramolecularly delivering a coordinated methoxide to the C═O unit; and (3) electrophilically assisting the departure of the leaving group amide anion.

Herein we report experimental details of the Cu(II)-promoted cleavage of a series of *N,N*-bis(2-picolyl) benzamides **4a−g** under ^s_spH-controlled[22] conditions along with supporting density functional theory (DFT) computations. This study complements and expands the communication of the methanolysis of **1**:Cu(II),[12] presenting additional details of the mechanism by providing the Hammett linear free energy relationship of log(k_x) vs σ_x for cleavage of various **4**:Cu(II), solvent kinetic isotope effects (SKIE) and activation parameters for the cleavage of representative examples **4b**:Cu(II) and **4g**:Cu(II), as well as a comparative DFT computational study for the cleavage of **4a**:Cu(II), **4b**:Cu(II), and **4g**:Cu(II).

2. RESULTS

a. Kinetics. The Cu(II)-promoted methanolysis of coordinated *N,N*-bis(2-picolyl) acetamide (**1**) exhibits a kinetic ^s_spK_a of 6.5 leading to a broad ^s_spH-insensitive region from 7 to 10 where the complex is in its basic active form, **1**:Cu(II):$(^-OCH_3)(HOCH_3)$.[12] With the expectation that the reactivity of **4**:Cu(II) has a similar sensitivity to ^s_spH as **1**:Cu(II), their methanolyses were studied at three ^s_spH values in the 7−8 plateau region of the ^s_spH/log(k_x) profile under buffered conditions (excess 2,4,6-collidine buffer) in the presence of excess Cu(II) (three concentrations of 1.0, 1.5, and 2.0 mM) to ensure that **4** is completely bound to Cu(II) during the reaction. The three rate constants (k_{obs}) for unimolecular decomposition of each complex, corrected for buffer and excess Cu(II) effects, were averaged to obtain k_x values. According to the mechanism depicted in Scheme 1, ionization of **4**:Cu(II):$(HOCH_3)_2$ generates the active form **4**:Cu(II):$(^-OCH_3)$-$(HOCH_3)$ which spontaneously decomposes. Given in Table 1 are the various k_x rate constants for the decomposition of **4a−g**:Cu(II):$(^-OCH_3)(HOCH_3)$ in the ^s_spH/log(k_x) plateau region from which a linear free energy relationship was constructed, correlating log(k_x) with the Hammett substituent constants, σ_x, as shown in Figure 1.

Table 1. Hammett Substituent Constants (σ_x) and Average Rate Constants (k_x) for the Decomposition of 4a−g:Cu(II):$(^-OCH_3)(HOCH_3)$ at 25.0 °C, Determined from Data at Three ^s_spH Values between 7 and 8

substrate	σ_x	10^4 k_x (s^{-1})[a]
4a	1.42	193 ± 40
4b	0.78	53 ± 2
4c	0.71	58 ± 6
4d	0.23	24.8 ± 0.7
4e	0.0	11 ± 1
4f	−0.17	11 ± 2
4g	−0.27	8.3 ± 0.5

[a]Determined as the average of three corrected rate constants (k_{obs}) for decomposition of **4a−g**:Cu(II):$(^-OCH_3)(HOCH_3)$ in the plateau rection in the ^s_spH/log(k_x) profile between 7 and 8.

Scheme 1. Simplified Scheme for the ^s_spH Dependent Decomposition of 4:Cu(II):$(^-OCH_3)(HOCH_3)$ to Form Cu(II):*N,N*-bis(2-picolyl)amine (Cu(II):DPA) and the Corresponding Methyl Benzoate (MB)

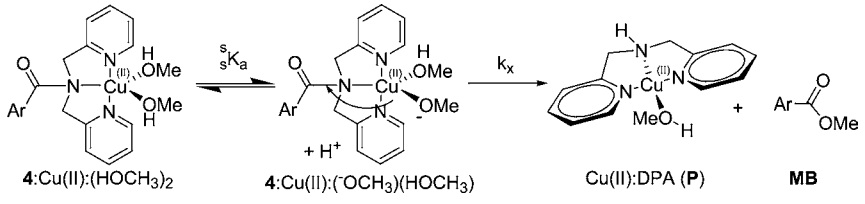

dx.doi.org/10.1021/ic301454y | Inorg. Chem. 2012, 51, 10325−10333

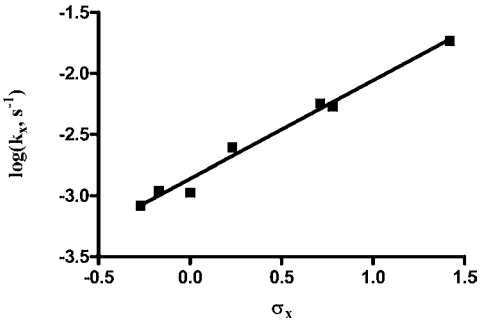

Figure 1. Hammett plot of $\log(k_x)$ vs σ_x for the Cu(II)-promoted cleavage of **4a−g** (5×10^{-4} M) in methanol at 25 °C in the plateau region (7−8) of the ${}^{s}_{s}$pH/$\log(k_x)$ profile. The line through the data is generated from a linear regression to provide $\rho_x = 0.80 \pm 0.05$; $r^2 = 0.9844$ (7 data).

b. Activation Parameters and Solvent Kinetic Isotope Effects. Experiments were carried out at five different temperatures in the plateau region of the ${}^{s}_{s}$pH/$\log(k_x)$ profiles for substrates **4b**:Cu(II):($^{-}$OCH$_3$)(HOCH$_3$) and **4g**:Cu(II):($^{-}$OCH$_3$)(HOCH$_3$). The respective Eyring plots at ${}^{s}_{s}$pH 7.0 ± 0.2 and 7.1 ± 0.2 are shown in Supporting Information, Figures 1S and 2S, while the corresponding activation parameters are given in Table 2. Also included in Table 2 are solvent deuterium kinetic isotope effects (SKIE) determined in triplicate for cleavage of **4b**:Cu(II):($^{-}$OCH$_3$)(LOCH$_3$) and **4g**:Cu(II):($^{-}$OCH$_3$)(LOCH$_3$) in CH$_3$OL (L = H, D) buffered with 2,4,6-collidine, (**4b**:Cu(II):($^{-}$OCH$_3$)(LOCH$_3$) ${}^{s}_{s}$pH = 7.1 ± 0.2, ${}^{s}_{s}$pD = 7.2 ± 0.2; **4g**:Cu(II):($^{-}$OCH$_3$)(LOCH$_3$) ${}^{s}_{s}$pH = 7.4 ± 0.2, ${}^{s}_{s}$pD = 7.4 ± 0.2). The ${}^{s}_{s}$pD values were measured at the end of the reactions in the same fashion as for ${}^{s}_{s}$pH; these are not corrected for the effect of the deuterated solvent on the ${}^{s}_{s}p$K$_a$ of the buffer or on the electrode readings. Since we are dealing with an extended plateau region of the ${}^{s}_{s}$pH/$\log(k_x)$ profiles, the actual ${}^{s}_{s}$pD values are less important since the rate constants in deuterated and proteated solvent are determined in the plateau region.

c. DFT Computations. The cleavage reactions of the Cu(II):($^{-}$OCH$_3$)(HOCH$_3$) complexes of **4a,b,g** were modeled using DFT to ascertain detailed mechanistic information and to correlate the computed energies of the transition states with their kinetic data. The starting ground state for each of the calculated pathways was the 5-coordinate monocationic complex [**4**:Cu(II):($^{-}$OCH$_3$)(HOCH$_3$)]$^{+}$. The primary goal of the calculations was to determine differences in relative free energies of the various transition states for each of the three substrates and their intermediates along the reaction pathway. Although the absolute values of the free energies of activation will be affected by the omission of explicit molecules of solvation, these were not included under the assumption that solvation should be similar for each substrate, and thus not important in determining the *differences* in energies between the same states of the three substrates. Geometry optimizations and energetic determinations for all intermediates and transition states were performed using the unrestricted B3LYP[23] functional employing the IEFPCM[24] continuum solvation model as implemented in the Gaussian 09 program.[25] The 6-31G(d,p) basis set was used for C and H; the 6-31++G(d,p) basis set was used for O and N; and the LANL2DZ[26] pseudopotential was used for Cu(II). Frequency calculations were conducted on optimized structures to determine free energy values at 298 K as well as to characterize intermediates and transition states. The lowest energy pathway for each amide is shown in Figure 2 and relevant structural data and activation parameters are shown Tables 3 and 4.

3. DISCUSSION

a. Lyoxide-Promoted Kinetics of Acyl Transfer. We first consider what is known about base-promoted acyl transfer from amides to solvent in the absence of metal-ion catalysts. The kinetics for alkaline hydrolysis of benzamides and toluamides[7,27] and those for anilides[28] as well as the basic methanolysis of anilides and benzamides[29] have received attention. In Scheme 2[30] is the general picture where there are

Scheme 2. Generalized Mechanism for the Base-Promoted Acyl Transfer of Amides

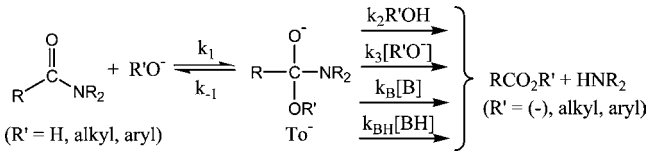

two primary steps for acyl transfer involving nucleophilic attack to form an anionic tetrahedral intermediate (T_O^-), followed by its breakdown to form the corresponding amine and carboxylate (if hydrolysis) or ester (if alcoholysis where R′ = alkyl or aryl). The latter step poses most of the interesting kinetic behavior since the departure of the leaving group often requires assistance from specific or general acids and bases. Schowen[31] reports that the kinetic rate law for basic hydrolysis of anilides has first and second order terms in [$^{-}$OH], and the rate-determining step changes with base concentration. Some simplification of the kinetics is seen in the methanolysis of anilides where the attacking CH$_3$O^{-} group precludes lyoxide deprotonation of T_O^- (R′ = CH$_3$) so the kinetics are simply first order in [$^{-}$OCH$_3$]. SKIE data for methanolysis indicate general acid assistance by the solvent for departure of the leaving group and, in certain cases, added buffers such as substituted phenols can also exert general assistance of the departure of the poor leaving group. Substituent effects exerted by Y-groups on the departing anilide (NRArY) show an increase in the amount of negative charge on the leaving group in the transition state for its departure as the substituents become more electron withdrawing ($\rho_y \sim 0$ for electron donors

Table 2. Activation Parameters, Rate Constants, and SKIE Values for Cleavage of [4b:Cu(II):($^{-}$OCH$_3$)(HOCH$_3$)]$^{+}$ and [4g:Cu(II):($^{-}$OCH$_3$)(HOCH$_3$)]$^{+}$ in Methanol at ${}^{s}_{s}$pH 7.0 ± 0.2 and 7.1 ± 0.2, Respectively, Determined in the Plateau Region of their ${}^{s}_{s}$pH/$\log(k_x)$ Profiles

substrate	k_x (s^{-1})	$\Delta H^{\ddagger}$ (kcal mol^{-1})	$\Delta S^{\ddagger}$ (cal mol^{-1} K^{-1})	$\Delta G^{\ddagger}$ (25 °C) (kcal mol^{-1})	k_H/k_D
[**4b**:Cu(II):($^{-}$OCH$_3$)(HOCH$_3$)]$^{+}$	3.9×10^{-3}	19.1 ± 0.2	−5.4 ± 0.6	20.7	1.12 ± 0.01
[**4g**:Cu(II):($^{-}$OCH$_3$)(HOCH$_3$)]$^{+}$	5.7×10^{-4}	21.3 ± 0.3	−2 ± 1	21.8	1.20 ± 0.02

dx.doi.org/10.1021/ic301454y | *Inorg. Chem.* 2012, 51, 10325−10333

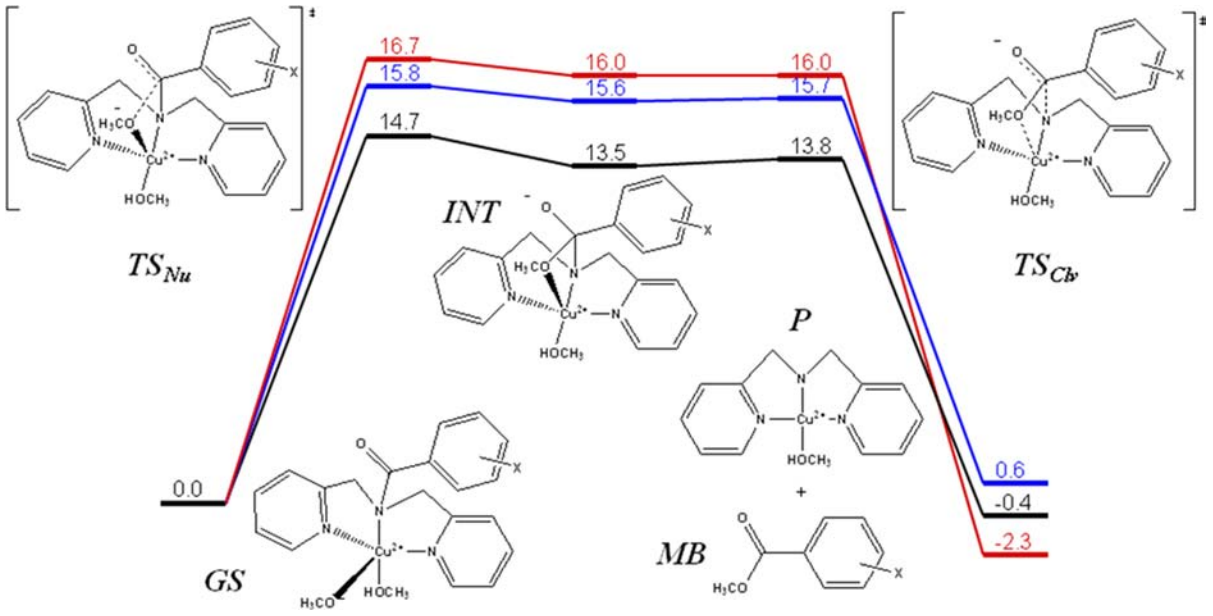

Figure 2. DFT-computed reaction pathway for the cleavage of the Cu(II):($^{-}OCH_3$)($HOCH_3$) complexes of **4a** (black); **4b** (blue); and **4g** (red) in methanol. All free energy values are to scale and are reported in kcal mol^{-1} at 298 K relative to the ***GS*** structure.

Table 3. Structural Data for DFT-Calculated Structures for the Cu(II):($^{-}OCH_3$)($HOCH_3$) Complexes of 4a,b,g[a]

Cu(II):($^{-}OCH_3$)($HOCH_3$) complex of **4a,b,g**		(Py)N-Cu(II)-N(Py)	χ_N[b]	Cu(II)-N_{trig} (Å)	Cu(II)-OCH_3 (Å)	$CH_3O^{-}C(=O)$ (Å)	N_{trig}-C(=O) (Å)
GS	**4a**	105.0°	150.1°	2.73	1.84	3.43	1.38
	4b	105.8°	149.6°	2.76	1.84	3.52	1.38
	4g	104.5°	154.1°	2.73	1.84	3.40	1.39
	1:Cu(II)	105.5°	152.6°	2.67	1.84	3.26	1.38
TS_{Nu}	**4a**	108.1°	132.9°	2.05	1.98	1.80	1.54
	4b	108.1°	132.9°	2.05	1.99	1.78	1.56
	4g	107.7°	132.6°	2.03	2.00	1.73	1.59
	1:Cu(II)	110.2°	136.5°	2.03	1.99	1.69	1.57
INT	**4a**	116.4°	133.1°	2.02	2.15	1.53	1.64
	4b	116.7°	132.7°	2.01	2.12	1.54	1.66
	4g	114.4°	132.6°	2.01	2.10	1.55	1.68
TS_{Clv}	**4a**	129.0°	129.2°	1.99	2.27	1.45	1.91
	4b	125.3°	130.1°	1.99	2.23	1.47	1.88
	4g	120.9°	130.7°	1.99	2.16	1.50	1.83
	1:Cu(II)	158.7°	131.8°	2.01	2.38	1.47	1.82
P^{+}		161.6°		1.97			
MB	**4a**					1.33	
	4b					1.34	
	4g					1.35	

[a]Structural information for **1**:Cu(II):($^{-}OCH_3$)($HOCH_3$) is taken from ref 12. [b]χ_N corresponds to the C−C−N-C(O) dihedral and is a measure of the trigonal nitrogen's pyramidalization that varies from 180° (sp^2 hybridization) and 120° (sp^3 hybridization). (Winkler, F. K.; Dunitz, J. D. *J. Mol. Biol.* **1971**, *59*, 169.)

like *p*-OCH_3 in the anilide ring, but ρ_y = 2.9 for withdrawers such as *m*-NO_2 or *p*-NO_2).

As we deal here with the cleavage of benzamides, it is relevant that Meloche and Laidler[27c] reported a Hammett ρ = 0.7 for hydroxide attack on some substituted benzamides at 100 °C in water. However, later $^{18}O{=}C$ exchange studies[27e] indicated that the ^{-}OH-promoted hydrolyses of benzamide, and to a lesser extent, N-methyl benzamide, but apparently not the tertiary *N*,*N*-dimethyl benzamide, suffer reversible formation of T_{O^-} (Scheme 2). Thus, Meloche's and Laidler's Hammett ρ-value, and related activation parameters, do not refer to a discrete kinetic step, but a complex term derived from Scheme 2 where $k_x = k_1[^{-}OH]k_2/(k_{-1} + k_2)$. Particularly relevant to the present work are the reports of Broxton and Deady on the basic methanolysis of N-methylbenzanilides[29f] and N-aryl-N-phenylbenzamides[29c] (**5**). Rate constants for methanolysis of compounds substituted in the benzoyl ring (i.e., X; Y = H) correlate well with σ_x (ρ_x = 1.76 (**5a**), 1.95 (**5b**)), indicative of a mechanism common to tertiary benzamides in methanol where the rate-limiting step is a solvent-assisted departure of the leaving group. This is generally confirmed by the Hammett plot of the rate constants for

dx.doi.org/10.1021/ic301454y | *Inorg. Chem.* 2012, 51, 10325−10333

Table 4. DFT-Calculated Activation Parameters for the Cleavage of the Cu(II):($^-OCH_3$)($HOCH_3$) Complexes of 4a,b,g (298 K, 1 atm)[a]

structure		$\Delta G^{\ddagger}$, kcal mol^{-1}	$\Delta H^{\ddagger}$, kcal mol^{-1}	$\Delta S^{\ddagger}$, cal mol^{-1} K^{-1}
TS_{Nu}	**4a**	14.7	11.8	−9.8
	4b	15.8	12.5	−11.1
	4g	16.7	13.2	−11.9
INT	**4a**	13.5	11.2	−7.8
	4b	15.6	12.2	−11.3
	4g	16.0	13.4	−8.7
TS_{Clv}	**4a**	13.8	11.2	−9.1
	4b	15.7	11.8	−13.0
	4g	16.0	13.5	−8.2

[a]All energies are relative to the respective *GS* structure.

compounds **5** substituted on the anilide ring (i.e., Y; X = H) which correlates well with σ_y (ρ_y = 2.5 (**5a**), 2.82 (**5b**)) in methanol, the large value of ρ_y being indicative of rate-limiting solvent-assisted departure of the LG (k_2(MeOH) in Scheme 2) where negative charge is building up on the anilide. Additional data from Broxton, Deady, and Rowe[29c] indicate that, as the amine leaving group gets better, k_2 increases and the rate-limiting step becomes nucleophilic attack.

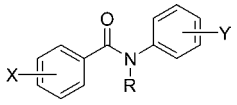

5a. R = Me
5b. R = Ph

b. Kinetics of Decomposition of 4:Cu(II):($^-OCH_3$)($HOCH_3$). The k_x data in Table 1 for the reaction of **4a−g** in the presence of Cu(II) ion refer to the unimolecular decomposition of **4**:Cu(II):($^-OCH_3$)($HOCH_3$). The experimental activation parameters for the *p*-nitro and *p*-methoxy derivatives [**4b**:Cu(II):($^-OCH_3$):($HOCH_3$)]$^+$ and [**4g**:Cu(II):($^-OCH_3$)($HOCH_3$)]$^+$ are, respectively, $\Delta H^{\ddagger}$, 19.1 and 21.3 kcal mol^{-1}, and $\Delta S^{\ddagger}$, −5.4 and −2 cal mol^{-1} K^{-1}. The reactions proceed readily at 25 °C, $t_{1/2}$ = ∼2 and 19 min respectively, indicating that the Cu(II) has a profound effect. A simple calculation indicates that the apparent second order rate constant for the reaction of CH_3O^- with **4b**:Cu(II):($HOCH_3$)$_2$ is 1.0 × 10^8 M^{-1} s^{-1}. This value is at least 2.0 × 10^{16} larger than the k_{MeO^-} for attack of methoxide on **4b** in the absence of the Cu(II).[32]

As was the case for the previously reported reaction of 1:Cu(II):($^-OCH_3$)($HOCH_3$),[12] the activation parameters and SKIE data of k_x^H/k_x^D of 1.1−1.2 observed here for decomposition of [**4b**:Cu(II):($^-OCH_3$)]$^+$ and [**4g**:Cu(II):($^-OCH_3$)($HOCH_3$)]$^+$ support a process of substantially rate-limiting, intramolecular nucleophilic attack of a Cu(II)-coordinated methoxide on the N-bound >N−C═O(Ar) unit. The Hammett ρ_x of 0.80 suggests a transition state where some negative charge is building up on the aromatic ring, but not as much as in the case of the methoxide-promoted methanolysis of the tertiary benzanilides, **5**. The fact that the plot in Figure 1 is linear, with no sign of an upward or downward break, suggests that there is no change in mechanism or rate-limiting step in passing through the members of series **4a−g**. The Hammett value can be compared to the ρ_x for attack of hydroxide on substituted methyl benzoate esters (2.2[33a]), hydroxide on benzamides (0.7[27b]), and methoxide on methyl aryl carbamates (2.15, 1.7[33b]) or benzanilides (1.76,[29f] 1.95[29c]) all of which show development of negative charge on the benzoyl group in the transition states. However, in addition to the solvent, nucleophile and substrate differences, none of the mechanisms operative in those systems is directly comparable to the mechanism for the decomposition of **4**:Cu(II):($^-OCH_3$)($HOCH_3$). This is made clearer by the additional information for the decomposition of the Cu(II) complexes derived from the computational data presented below.

c. DFT Computational Studies. The lowest energy pathways computed for the cleavage reactions of **4a,b,g**:Cu(II):($^-OCH_3$)($HOCH_3$) are shown in Figure 2 with the relevant structural data and activation parameters given in Tables 3 and 4. Several possible ground state structures were calculated, and the lowest energy complex found was the trigonal bipyramidal Cu(II):($^-OCH_3$)-containing structure labeled as *GS* having the pyridine moieties and methoxide occupying equatorial positions. In *GS*, the aryl ring is coplanar with the adjacent C═O bond. All free energy values are reported relative to the free energy of this structure. The amide nitrogen geometry in this structure suggests a degree of Cu(II)−N_{amidic} interaction, however to a lesser extent than is shown with the corresponding acyl structure, **1**:Cu(II):($^-OCH_3$)($HOCH_3$) as judged from the Cu(II)−N_{amidic} distance[12] (2.73−2.76 Å vs 2.67 Å).

Nucleophilic attack proceeds via closure of the amidic O═C---$^-OCH_3$:(Cu(II)) bond distance in TS_{Nu}, and is associated with free energies of 14.7 kcal mol^{-1} (**4a**), 15.8 kcal mol^{-1} (**4b**), and 16.7 kcal mol^{-1} (**4g**). The O═C---$^-OCH_3$ interatomic distances given in Table 3 for TS_{Nu} vary from 1.80 Å (**4a**) to 1.73 Å (**4g**), indicating tighter transition states and higher transition state energies with more electron-donating aryl substituents. For each **4** tested, there is a larger degree of Cu(II)−N_{amidic} interaction during nucleophilic attack, as indicated by a shortening of that bond (from 2.73−2.76 Å to 2.03−2.05 Å) and an increase in nitrogen pyramidalization (χ_N decreases from ∼150−154° to 132.6−132.9°; Table 3). The TS_{Nu} structure leads to a single tetrahedral intermediate structure *INT*, which occupies a shallow minimum on the free energy surface. This can be contrasted with the previously reported[12] DFT-calculated mechanism for the breakdown of the acetyl derivative **1**:Cu(II):($^-OCH_3$)($HOCH_3$) which was found to involve two sequential tetrahedral intermediates separated by a transition state that largely involved the rearrangement of the ligands about the Cu(II). Such a rearrangement of the ligands around the Cu(II) in **4** does not appear to be operative, as there is a single *INT* that rapidly progresses to product through TS_{clv} where the latter involves departure of the amide anion coordinated to Cu(II). This may be a consequence of a destabilization of the equivalent planar Cu(II) intermediate (Structure INT_3 in ref 12) because of the unfavorable steric interaction caused by the bulkier aryl benzamide moiety relative to the smaller acetamide. The *INT* breakdown is virtually barrierless, involving a shortening of the Cu(II)-trigonal N bond distance by 0.02−0.03 Å to 1.99 Å for **4b,g** and **4a** with concurrent planarization of the Cu(II) (opening of the (Py)N−Cu(II)−N(Py) angle). The trigonal N−C(═O) interatomic distance lengthens in TS_{clv}, varying from 1.91 Å (**4a**) to 1.83 Å (**4g**), indicative of later transition states for benzamides containing more electron withdrawing groups. The square planar product structure (*P*) follows this transition state; the (Pyr-CH_2)$_2N^-$---Cu(II) departs without N-protonation, but having departed, is assumed to be rapidly protonated under the reaction conditions.

dx.doi.org/10.1021/ic301454y | *Inorg. Chem.* 2012, 51, 10325−10333

d. Computed Hammett Plot. The computed mechanisms for all substrates reveal that the rate-determining process is the intramolecular nucleophilic attack of the Cu(II)-coordinated methoxide on the C═O unit. Where a direct comparison can be made for [**4b**:Cu(II):($^-$OCH$_3$)(HOCH$_3$)]$^+$ and [**4g**:Cu(II):($^-$OCH$_3$)(HOCH$_3$)]$^+$, the computed free energies (Table 4) are less than those determined experimentally by 3.4 and 4.6 kcal mol^{-1}. The differences are likely due to the absence of explicit solvent−solute interactions in the calculated process, specifically in desolvating the nucleophilic methoxide, and resolvating the developing C−O$^-$ in ***TS***$_{Nu}$. Since all the substrates should experience similar desolvation/resolvation, or ones that change regularly with the electron withdrawing nature of the substituent on Ar, we assume these can be omitted leaving the differences in free energy of activation of the three computed species as being more representative of the process at hand. Indeed, the DFT calculated free energies for the structures are used to construct a Hammett Plot (Supporting Information, Figure 2S) with ρ_x = 0.84 ± 0.16, which is the same as the experimental value of 0.80 ± 0.05.

4. CONCLUSIONS

The present, and earlier, studies[12−17] indicate that poorly reactive amides having O═C−N(Lig)$_2$ units that bind metal ions such as Cu^{2+} become unusually reactive toward methanolysis of their metal-complexes at room temperature and neutral ^s_spH. The close positioning of Cu(II) to the amidic N of a N−C═O unit permits several catalytic roles for the metal ion. Some of these are common to metal ion-catalyzed solvolytic cleavage of other systems, such as (1) positioning a nucleophilic lyoxide and a bound substrate to a metal ion closely enough for reaction; (2) reduction of the pK_a of a metal-bound solvent molecule so that it becomes the preferred nucleophile; and (3) electrostatic stabilization by the metal ion of a developing anionic ***TS***$_{Nu}$. The present system exhibits unusual modes of the Cu(II) interaction with the ***TS***$_{Nu}$ that are rarely observed in metal ion-catalyzed solvolyses, possibly because of the difficulty in positioning the metal ion, in small molecule examples, to enable coordination with the amidic N. With substrates such as **1** and **4** there is an enforced Cu(II) interaction with the amidic N-lone pair that decouples its conjugation with the adjacent C═O. This is an alternative to the usual Lewis acid M(II)---O═C interaction; the present work shows that both types can activate the amide toward nucleophilic attack. A referee[34] has offered that this mode of binding of the Cu(II) to the amidic N activates the substrate for the initial steps of the reaction because it renders the system more like an acylammonium[35] than a regular amide. Because the binding of the metal ion to amides **4** and **1** is relatively strong, the reduction of amidic resonance stabilization (as measured by the decrease in the barrier to rotation[36] or effects on solvolytic reactivity) is brought about by utilizing the binding energy of the Cu(II) to the two 2-picolyl groups. However, according to the DFT computed rotational barriers for **4b** and **4b**:Cu(II):($^-$OMe)(HOMe) as well as **1** and **1**:Cu(II):($^-$OMe)(HOMe), there is only a 3.4 and 4.9 kcal/mol reduction of the rotational barrier in the Cu(II) complexes.[37] This is consistent with the experimental results for Lectka et al.[36] and suggests that the Cu(II) binding to substrate does not reduce the amidic resonance nearly as much as would be anticipated by an acylammonium analogue. Nevertheless, the very large acceleration of the methanolytic reaction provides a small-molecule example supporting the hypothesis that, for enzyme-catalyzed acyl transfer reactions of peptides, a portion of the exothermicity of substrate binding is utilized in a productive way by the enzyme to destabilize and thereby activate the scissile substrate bond as the transition state for the acyl transfer reaction is approached.[38]

A subsequent important role of the metal ion in this system is to assist the departure of the LG via Lewis acid coordination to the developing amide anion, thereby lowering the transition state energy for the cleavage of the tetrahedral intermediate. This is an additional important aspect for a two-step, metal ion-catalyzed process where the metal ion must promote both the addition and the breakdown steps, fulfilling a multifunctional role. This sort of interaction is likely to be an important phenomenon in enzyme-catalyzed hydrolytic or alcoholytic cleavage of substrates with poor leaving groups where electrophilic assistance must be given to enhance both nucleophilic attack and LG departure.

According to the principles of enzyme catalysis first enunciated by Pauling,[39] "the enzyme has a configuration complementary to the activated complex, and accordingly has the strongest power of attraction for the activated complex." Extending this leads to the widely held notion that good catalysts bind transition states stronger than they bind ground states. Furthermore, for any catalyst promoting a multistep reaction, each of the steps must be lowered in energy to achieve the overall high rates for the catalytic reaction. Zhang and Houk have recently analyzed[40] a large number of enzymatic systems, concluding that the very best catalytic systems have a transition state binding energy well in excess of what can be achieved by noncovalent interactions. That proficiency arises from additional covalent effects such as heavy atom- and H-bond formation, and strong interactions of cofactors such as metal ions with transforming substrates that develop between the enzyme (catalyst) and transition state, thereby altering the mechanism from what is seen in the absence of catalyst. It is an interesting observation that this sort of covalent bonding is manifested in the way the Cu(II) binds the transition states for the two-step solvolysis reaction described herein, and in other systems we have reported for efficient alcoholysis of phosphorothioates[41] and thioamides[42] promoted by a simple palladacycle. These types of interactions should be manifested in other systems where ligands are bound to departing groups so that a metal ion can facilitate the solvolytic cleavage of amides, esters, carbamates, phosphates, phosphoramidates, and sulfates in such a way that they may prove more generally useful in synthetic applications.

5. EXPERIMENTAL SECTION

a. Materials. Methanol (99.8%, anhydrous) and acetonitrile (99.8%, anhydrous) were purchased from EMD Chemicals. Trifluoromethanesulfonic acid (HOTf, ≥99%), methanol-OD (99.5 atom % D), 2-pyridinecarboxaldehyde (99%), 2-aminomethylpyridine (98%), 4-nitrobenzoyl chloride (98%), benzoyl chloride (99%), 4-methoxybenzoyl chloride (99%), 3,5-dinitrobenzoyl chloride (98+%), 4-chlorobenzoyl chloride (99%), 4-toluoyl chloride (98%), 3-nitrobenzoyl chloride (98%), and triethylamine (99%) were obtained from Aldrich. Chloroform-*d* (99.8% D), methylene chloride-d_2 (99.9% D), and Cu(OTf)$_2$ (98%) were obtained from TCI America Laboratory Chemicals; 2,4,6-collidine (98%) was obtained from BDH Laboratory Reagents.

b. General Methods. All ^{1}H NMR spectra were determined at 400 MHz and ^{13}C NMR spectra at 100.58 MHz. All high-resolution mass spectra were determined by ESI-TOF. $CH_3OH_2^+$ concentrations were determined potentiometrically using a combination glass Fisher

dx.doi.org/10.1021/ic301454y | Inorg. Chem. 2012, 51, 10325−10333

Scientific Accumet electrode model no. 13-620-292 calibrated with certified standard aqueous buffers (pH 4.00 and 10.00) as described previously.[43] The $^{s}_{s}$pH values in methanol were determined by subtracting a correction constant of −2.24[22] from the electrode readings and the autoprotolysis constant for methanol was taken to be $10^{-16.77}$ M^2. The $^{s}_{s}$pH values for the kinetic experiments were measured at the end of the reactions to avoid the effect of KCl leaching from the electrode.

c. Synthesis of Materials, Dipicolylamine (*N,N*-bis(2-picolyl)-amine) and 4a−g. *5.c.1. N,N-bis(2-picolyl)amine or Dipicolylamine.* A modification of the literature procedure was used.[44] To a solution of 2-pyridinecarboxaldehyde (4.44 mL, 46 mmol) in dry MeOH (150 mL) was added 2-aminomethylpyridine (4.76 mL, 46 mmol) at room temperature (RT) after which the brown mixture was stirred for 5 h. Sodium borohydride (3.5 g, 92 mmol) was added in small portions with stirring, maintaining the reaction at 0 °C using an ice bath. The mixture changed color from brown to yellow and was stirred for 15 h at room temperature. Conc. HCl was added slowly to adjust the pH to 1, and the solution was stirred for 2 h. Next, a saturated solution of NaOH was added to adjust the pH to 11. The reaction mixture was filtered, and the solvent was removed under vacuum. Water was added to the residue; the aqueous mixture was extracted twice with CH_2Cl_2, and the combined extracts dried over anhydrous magnesium sulfate and filtered. The solvent was removed under vacuum. The product was obtained as a brown oil in 85% yield (7.78 g, 39.1 mmol).

HRMS: calculated for $C_{12}H_{13}N_3$ 199.1109 amu, found 199.1102 amu; ^{1}H NMR (CD_2Cl_2, 25 °C): δ 2.37 (bs, 1H), 3.91 (s, 4H), 7.13−7.16 (m, 2H), 7.33 (d, J = 8.11 Hz, 2H), 7.63 (td, $J1$ = 7.67 Hz, $J2$ = 16.69 Hz, 2H), 8.51 (d, J = 4.91 Hz, 2H); ^{13}C NMR (CD_2Cl_2, 25 °C): δ 55.0, 122.3, 122.5, 136.7, 149.5, 160.3.

*5.c.2. 4-Nitro-N,N-bis(2-picolyl)benzamide (**4b**).* To a solution of dipicolylamine (1.5 g, 7.53 mmol) in CH_2Cl_2 was slowly added 4-nitrobenzoyl chloride (1.7 g, 9.16 mmol) and triethylamine (1.27 mL, 9.16 mmol). The mixture was refluxed for 3.5 h then stirred for 2 h at room temperature. The reaction mixture was washed with water (2×), saturated sodium carbonate solution (2×), and finally with water (2×), then dried over anhydrous $MgSO_4$. The CH_2Cl_2 was removed under vacuum, and the crude product was purified by column chromatography on silica gel using CH_2Cl_2/MeOH (90:10) as the eluent. The solvent was removed under vacuum, and the resulting solid was recrystallized in anhydrous ethyl ether and ethyl acetate. The product was obtained as fine pale yellow needles in 75% yield (1.97 g, 5.65 mmol).

HRMS: calculated for $C_{19}H_{16}N_4O_3$ 348.1222 amu, found 348.1231 amu; ^{1}H NMR (CD_2Cl_2, 25 °C): δ 4.59 (s, 2H), 4.80 (s, 2H), 7.11 (d, J = 7.80 Hz, 1H), 7.20−7.24 (q, 2H), 7.36 (d, J = 7.80 Hz, 1H), 7.64−7.72 (m, 2H), 7.77 (d, J = 8.98 Hz, 2H), 8.19 (d, J = 8.99 Hz, 2H), 8.53 (d, J = 4.70 Hz, 1H), 8.60 (d, J = 4.70 Hz, 1H); ^{13}C NMR ($CDCl_3$, 25 °C): δ 50.4, 54.1, 121.9, 122.5, 122.78, 122.82, 123.6, 128.3, 136.8, 142.3, 149.4, 150.0, 155.6, 156.5, 170.4; $\varepsilon_{260\ nm}$ = 14940 ± 90 M^{-1} cm^{-1}; melting point: 95 °C.

*5.c.3. 3,5-Dinitro-N,N-bis(2-picolyl)benzamide (**4a**).* This compound was synthesized from dipicolylamine (1 g, 5.02 mmol), 3,5-dinitrobenzoyl chloride (1.38 g, 6.02 mmol), and triethylamine (0.84 mL, 6.02 mmol) using a procedure similar to that above for the preparation of 4-nitro-*N,N*-bis(2-picolyl)benzamide. The compound was obtained as pale yellow needles in 68% yield (1.34 g, 3.42 mmol).

HRMS: calculated for $C_{19}H_{15}N_5O_5$ 393.1073 amu, found 393.1065 amu; ^{1}H NMR (CD_2Cl_2, 25 °C): δ 4.61 (s, 2H), 4.78 (s, 2H), 7.15 (d, J = 7.50 Hz, 1H), 7.22−7.29 (m, 2H), 7.38 (d, J = 7.79 Hz, 1H), 7.67−7.73 (q, 2H), 8.55 (d, J = 3.90 Hz, 1H), 8.69 (d, J = 3.90 Hz, 1H), 9.02−9.04 (m, 3H); ^{13}C NMR (CD_2Cl_2, 25 °C): δ 51.1, 119.8, 123.0, 123.1, 123.2, 123.6, 128.7, 137.2, 137.3, 140.3, 148.8, 149.8, 150.5, 155.5, 156.7, 168.1; $\varepsilon_{235\ nm}$ = 20390 ± 651 M^{-1} cm^{-1}; melting point: 120 °C.

*5.c.4. 3-Nitro-N,N-bis(2-picolyl)benzamide (**4c**).* This compound was synthesized from dipicolylamine (1 g, 5.02 mmol), 3-nitrobenzoyl chloride (1.12 g, 6.02 mmol), and triethylamine (0.84 mL, 6.02 mmol) using a procedure similar to that above for the preparation of 4-nitro-*N,N*-bis(2-picolyl)benzamide.. The compound was obtained as a brown oil in 80% yield (1.40 g, 4.02 mmol).

HRMS: calculated for $C_{19}H_{16}N_4O_3$ 348.1222 amu, found 348.1231 amu; ^{1}H NMR (CD_2Cl_2, 25 °C): δ 4.62 (s, 2H), 4.80 (s, 2H), 7.13 (d, J = 7.48, 1H), 7.21−7.25 (q, 2H), 7.38 (d, J = 7.18 Hz, 1H), 7.57 (t, 1H), 7.66−7.72 (q, 2H), 7.96 (dt, Jd = 1.55 Hz, Jt = 7.58 Hz, 1H), 8.21−8.24 (dq, Jq = 4.80 Hz, 1H), 8.52 (t, 1H), 8.54 (d, J = 4.05 Hz, 1H), 8.62 (d, J = 3.75 Hz, 1H); ^{13}C NMR (CD_2Cl_2, 25 °C): δ 50.9, 54.6, 122.4, 122.8, 122.9, 123.2, 124.6, 130.0, 133.7, 137.07, 137.13, 138.4, 148.4, 149.7, 150.3, 156.3, 157.2, 170.2; $\varepsilon_{260\ nm}$ = 9233 ± 193 M^{-1} cm^{-1}.

*5.c.5. 4-Chloro-N,N-bis(2-picolyl)benzamide (**4d**).* This compound was synthesized from dipicolylamine (1 g, 5.02 mmol), 4-chlorobenzoyl chloride (1.05 g, 6.02 mmol) and triethylamine (0.84 mL, 6.02 mmol) using a procedure similar to that above for the preparation of 4-nitro-*N,N*-bis(2-picolyl)benzamide. The compound was obtained as pale yellow needles in 45% yield (0.76 g, 2.26 mmol).

HRMS: calculated for $C_{19}H_{16}N_3OCl$ 337.0982 amu, found 337.0975 amu; ^{1}H NMR (CD_2Cl_2, 25 °C): δ 4.63 (s, 2H), 4.78 (s, 2H), 7.14 (d, J = 7.52 Hz, 1H), 7.21 (bs, 2H), 7.33 (d, J = 8.59 Hz, 3H), 7.52 (d, J = 8.59 Hz, 2H), 7.68 (bs, 2H), 8.52 (d, J = 2.50 Hz, 1H), 8.58 (d, J = 2.70 Hz, 1H); ^{13}C NMR (CD_2Cl_2, 25 °C): δ 50.7, 54.8, 122.1, 122.7, 122.9, 128.9, 129.0, 135.2, 135.9, 137.0, 149.6, 150.2, 156.8, 157.5, 171.6; $\varepsilon_{260\ nm}$ = 13490 ± 172 M^{-1} cm^{-1}; melting point: 73 °C.

*5.c.6. N,N-bis(2-picolyl)benzamide (**4e**).*[14] This was synthesized from dipicolylamine (1.42 g, 7.13 mmol), benzoyl chloride (1.20 g, 8.56 mmol) and triethylamine (1.20 mL, 8.56 mmol) using a procedure similar to that above for the preparation of 4-nitro- *N,N*-bis(picolyl)benzamide. The crude product was purified by column chromatography on silica gel using EtOAc/MeOH (95:5) as the eluent. The compound was obtained as a pale yellow solid in 65% yield (1.40 g, 4.63 mmol).

HRMS: calculated for $C_{19}H_{17}N_3O$ 303.1372 amu, found 303.1359 amu; ^{1}H NMR (CD_2Cl_2, 25 °C): δ 4.65 (s, 2H), 4.80 (s, 2H), 7.15−7.21 (m, 3H), 7.33−7.40 (m, 4H), 7.51−7.54 (m, 2H), 7.64−7.69 (m, 2H), 8.52 (d, J = 12.25 Hz, 2H); ^{13}C NMR (CD_2Cl_2, 25 °C): δ 50.7, 54.9, 122.0, 122.6, 122.8, 127.3, 128.7, 129.9, 136.8, 137.0, 149.7, 150.2, 157.2, 157.7, 172.6; $\varepsilon_{260\ nm}$ = 8289 ± 137 M^{-1} cm^{-1}; melting point: 66 °C.

*5.c.7. 4-Methyl-N,N-bis(2-picolyl)benzamide (**4f**).* This compound was synthesized from dipicolylamine (1 g, 5.02 mmol), *p*-toluoyl chloride (0.93 g, 6.02 mmol), and triethylamine (0.84 mL, 6.02 mmol) using a procedure similar to that above for the preparation of 4-nitro-*N,N*-bis(2-picolyl)benzamide. The crude product was purified by column chromatography on silica gel using EtOAc/MeOH (95:5) as the eluent. The compound was obtained as fine white needles in 76% yield (1.21 g, 3.82 mmol).

HRMS: calculated for $C_{20}H_{19}N_3O$ 317.1528 amu, found 317.1519 amu; ^{1}H NMR (CD_2Cl_2, 25 °C): δ 2.34 (s, 3H), 4.67 (s, 2H), 4.79 (s, 2H), 7.16−7.21 (m, 5H), 7.37 (d, J = 6.72 Hz, 1H), 7.41 (d, J = 8.07 Hz, 2H), 7.68 (t, 2H), 8.52 (d, J = 12.88 Hz, 2H); ^{13}C NMR (CD_2Cl_2, 25 °C): δ 21.5, 50.7, 54.9, 121.8, 122.5, 122.8, 127.3, 129.3, 133.7, 137.0, 140.3, 149.6, 150.1, 172.7; $\varepsilon_{255\ nm}$ = 8911 ± 44 M^{-1} cm^{-1}; melting point: 103 °C.

*5.c.8. 4-Methoxy-N,N-bis(2-picolyl)benzamide (**4g**).* This was synthesized from dipicolylamine (1.52 g, 7.63 mmol), 4-methoxybenzoyl chloride (1.56 g, 9.15 mmol), and triethylamine (1.27 mL, 9.15 mmol) using a procedure similar to that above for the preparation of 4-nitro-*N,N*-bis(picolyl)benzamide. The crude product was purified by column chromatography on silica gel using EtOAc/MeOH (90:10) as the eluent. The compound was obtained as fine white needles in 55% yield (1.4 g, 4.20 mmol).

HRMS: calculated for $C_{20}H_{19}N_3O_2$ 333.1477 amu, found 333.1471 amu; ^{1}H NMR (CD_2Cl_2, 25 °C): δ 3.80 (s, 3H), 4.75 (bs, 4H), 6.86 (d, J = 8.76 Hz, 2H), 7.20 (t, 3H), 7.36 (s, 1H), 7.51 (d, J = 8.77 Hz, 2H), 7.68 (td, $J1$ = 7.76 Hz, $J2$ = 17.03 Hz, 2H), 8.55 (bs, 2H); ^{13}C NMR (CD_2Cl_2, 25 °C): δ 55.7, 113.9, 122.6, 128.7, 129.3, 137.0, 161.2, 172.7; $\varepsilon_{255\ nm}$ = 15190 ± 620 M^{-1} cm^{-1}; melting point: 83 °C.

dx.doi.org/10.1021/ic301454y | *Inorg. Chem.* 2012, 51, 10325−10333

d. General UV−vis Kinetics. The Cu(II)-catalyzed methanolyses of the Cu(II):($^{-}OCH_3$)($HOCH_3$) complexes of **4a−g** were followed at 360 nm for the disappearance of the **4**:Cu(II):($^{-}OCH_3$)($HOCH_3$) complex using a UV−vis spectrophotometer with the cell compartment thermostatted at 25.0 ± 0.1 °C. The reactions were conducted in the presence of buffers composed of various ratios of 2,4,6-collidine and HOTf ($_s^s$pH 7.2, 7.6, and 7.9) to maintain the $_s^s$pH in methanol. A typical kinetic experiment involved preparing a methanol solution containing buffer (10−20 mM) and Cu(II) (1.0−2.0 mM) in a 1 cm path length quartz cuvette. Initiation of the reaction involved addition of an aliquot of the preformed **4**:Cu(II) complex (0.5 mM) in acetonitrile to the buffered methanol solution to achieve the desired concentrations of the reaction components in a final volume of 2.5 mL. The absorbance vs time traces were fit to a standard first order exponential equation to obtain the observed first order rate constants (k_{obs}). The rate constants for the methanolysis of **4**:Cu(II):($^{-}OCH_3$) in the presence of excess Cu(II), required to ensure complete binding, exhibited small buffer and Cu(II) concentration effects. The observed k_{obs} values were extrapolated to zero buffer concentration for each [$Cu(OTf)_2$] using three buffer concentrations (10 mM, 15 mM, 20 mM). These extrapolated values were then extrapolated to zero excess Cu(II) using two or three excess Cu(II) concentrations (1.0 mM, 1.5 mM, 2.0 mM) to provide corrected rate constants for a given $_s^s$pH. Averages of the three rate constants for a given substrate (k_x) are presented in Table 1.

e. Product Analysis. The methanolysis of **4b**:Cu(II):($^{-}OCH_3$)($HOCH_3$) and **4g**:Cu(II):($^{-}OCH_3$)($HOCH_3$) were conducted at higher concentration in CH_3OH (10 mM 2,4,6-collidine buffer, 4 mM Cu(II), 3 mM **4b,g**). After completion of the reaction (assessed by UV−vis spectroscopy), the solvent was evaporated using a rotary evaporator, redissolved in $CDCl_3$, and the ^{1}H NMR spectrum at 400 MHz was collected. The only observable product in each case was the corresponding methyl benzoate. The Cu(II) complex of *N*,*N*-bis(2-picolyl)amine was not observed by ^{1}H NMR because of Cu(II)-induced paramagnetic broadening.

f. Solvent Kinetic Isotope Effect (SKIE) Experiments. The SKIE experiments for Cu(II)-assisted cleavage of **4b**:Cu(II):($^{-}OCH_3$)($HOCH_3$) and **4b**:Cu(II):($^{-}OCH_3$)($HOCH_3$) involved the addition of 2,4,6-collidine buffer, Cu(II), and **4b,g**:Cu(II) to UV cells containing either CH_3OH or CH_3OD so that the final concentrations of buffer, Cu(II), and substrate were 10 mM, 1.5 mM, and 0.5 mM. Triplicate competition experiments were done, and the $_s^s$pH and $_s^s$pD values were measured at the end of the reactions (**4b**:Cu(II); $_s^s$pH = 7.1 ± 0.2, $_s^s$pD = 7.2 ± 0.2; **4g**:Cu(II); $_s^s$pH = 7.4 ± 0.2, $_s^s$pD = 7.4 ± 0.2).

g. Activation Parameters. Kinetic experiments with **4b**:Cu(II):($^{-}OCH_3$)($HOCH_3$) and **4g**:Cu(II):($^{-}OCH_3$)($HOCH_3$) were conducted at five different temperatures from 15.0 to 55.1 °C using a UV−vis spectrophotometer with a thermostatted cell holder. Solution temperatures were determined using a dummy cell adjacent to the reaction cell into which a thermometer was inserted before and after the reaction. First order rate constants were determined in triplicate for 0.5 mM **4b**:Cu(II):($^{-}OCH_3$)($HOCH_3$) and **4g**:Cu(II):($^{-}OCH_3$)($HOCH_3$) along with 1.0 mM excess Cu(II) in the presence of 10 mM collidine buffer, $_s^s$pH 7.0 ± 0.2. Eyring plots of ln(k/T) vs 1/T shown in the Supporting Information, Figures 1S and 2S provided the $\Delta H^{\ddagger}$ and $\Delta S^{\ddagger}$ values given in Table 2.

■ ASSOCIATED CONTENT

Supporting Information

NMR characterization of compounds **4a−d,f,g**, Eyring plots for the cleavage of **4b**:Cu(II):($^{-}OCH_3$)($HOCH_3$) and **4g**:Cu(II):($^{-}OCH_3$)($HOCH_3$) in methanol, pseudo-first order rate constants, extrapolated rate constants for the methanolysis of **4a−g**:Cu(II):($^{-}OCH_3$)($HOCH_3$) in the presence of multiple concentrations of buffers and [Cu(II)] at 25 °C, DFT optimized atomic coordinates for all structures, and the complete citation for reference 25, 29 pages. This material is available free of charge via the Internet at http://pubs.acs.org.

■ AUTHOR INFORMATION

Corresponding Author

*E-mail: rsbrown@chem.queensu.ca. Phone: 613-533-2400. Fax: 613-533-6669.

Notes

The authors declare no competing financial interest.

■ ACKNOWLEDGMENTS

The authors gratefully acknowledge the generous support of the Natural Sciences and Engineering Research Council of Canada (NSERC) and Queen's University. In addition, M.A.R.R. thanks the Government of Ontario and Queen's University for a QEII-GSST. R.A.A.O. also thanks the Government of Ontario and Queen's University for the award of a 2012 Summer Work Experience Program (SWEP) stipend.

■ REFERENCES

(1) (a) Brown, R. S.; Neverov, A. A. *J. Chem. Soc. Perkin 2.* **2002**, 1039. (b) Brown, R. S.; Neverov, A. A.; Tsang, J. S. W.; Gibson, G. T. T.; Montoya-Peláez, P. J. *Can. J. Chem.* **2004**, *82*, 1791. (c) Brown, R. S.; Neverov, A. A. *Adv. Phys. Org. Chem.* **2008**, *42*, 271. (d) Brown, R. S.; Lu, Z.-L.; Liu, C. T.; Tsang, W. Y.; Edwards, D. R.; Neverov, A. A. *J. Phys. Org. Chem.* **2009**, *23*, 1 and references therein.

(2) Brown, R. S. In *Progress in Inorganic Chemistry*; Karlin, K., Ed.; John Wiley and Sons: New York, 2011 Vol. *57*, p 55, and references therein.

(3) (a) Williams, N. H.; Takasaki, B.; Wall, M.; Chin, J. *Acc. Chem. Res.* **1999**, *32*, 485. (b) Morrow, J. *Comments Inorg. Chem.* **2008**, *29*, 169. (c) Fothergill, M.; Goodman, M. F.; Petruska, J.; Warshel, A. *J. Am. Chem. Soc.* **1995**, *117*, 11619. (d) Richard, J. P.; Amyes, T. L. *Bioorg. Chem.* **2004**, *32*, 354.

(4) Liu, C. T.; Neverov, A. A.; Maxwell, C. I.; Brown, R. S. *J. Am. Chem. Soc.* **2010**, *132*, 3561.

(5) Rawlings, N. D.; Barrett, A. J. Introduction: metallopeptidases and their clans. In *Handbook of Proteolytic Enzymes*, 2nd ed.; Barrett, A. J., Rawlings, N. D., Woessner, J. F., Eds.; Academic: Oxford, U.K., **2004**; Vol. *1*, p 231.

(6) (a) Polzin, G. M.; Burstyn, J. N. *Met. Ions Biol. Syst.* **2001**, *38*, 103. (b) Fife, T. H.; Bembi, R. *J. Am. Chem. Soc.* **1994**, *115*, 11358. (c) Schepartz, A.; Breslow, R. *J. Am. Chem. Soc.* **1987**, *109*, 1814. (d) Suh, J.; Moon, S.-J. *Inorg. Chem.* **2001**, *40*, 4890. (e) Neverov, A. A.; Montoya-Pelaez, P. J.; Brown, R. S. *J. Am. Chem. Soc.* **2001**, *123*, 210. (f) Neverov, A. A.; Brown, R. S. *Can. J. Chem.* **2000**, *78*, 1247 and references therein.

(7) Brown, R. S.; Bennet, A. J.; Slebocka-Tilk, H. *Acc. Chem. Res.* **1992**, *25*, 481.

(8) Stoffregen, S. A.; Griffin, A. K. K.; Kostic, N. M. *Inorg. Chem.* **2005**, *44*, 8899 and references therein..

(9) Milovic, N. M.; Badjic, J. D.; Kostic, N. M. *J. Am. Chem. Soc.* **2004**, *126*, 696.

(10) (a) Somayaji, V.; Brown, R. S. *J. Org. Chem.* **1986**, *51*, 2676. (b) Wang, Q.-P.; Bennet, A. J.; Brown, R. S.; Santarsiero, B. D. *Can. J. Chem.* **1990**, *68*, 1732. (c) Wang, Q.-P.; Bennet, A. J.; Brown, R. S.; Santarsiero, B. D. *J. Am. Chem. Soc.* **1991**, *113*, 5757. (d) Slebocka-Tilk, H.; Brown, R. S. *J. Org. Chem.* **1987**, *52*, 805.

(11) Montoya-Pelaez, P.; Gibson, G. T. T.; Neverov, A. A.; Brown, R. S. *Inorg. Chem.* **2004**, *42*, 8624.

(12) Barrera, I. F.; Maxwell, C. I.; Neverov, A. A.; Brown, R. S. *J. Org. Chem.* **2012**, *77*, 4156.

(13) Houghton, R. P.; Puttner, R. R. *Chem. Commun.* **1970**, 1270.

(14) Niklas, N.; Heinemann, F. W.; Hampel, F.; Clark, T.; Alsfasser, R. *Inorg. Chem.* **2004**, *43*, 4663 , and references therein.

(15) Niklas, N.; Alsfasser, R. *Dalton Trans.* **2006**, 3188.
(16) Bröhmer, M. C.; Bannwarth, W. *Eur. J. Org. Chem.* **2008**, 4412.
(17) Bröhmer, M. C.; Mundinger, S.; Bräse, S.; Bannwarth, W. *Angew. Chem.* **2011**, *50*, 6125.
(18) (a) Szajna-Fuller, E.; Ingle, G. K.; Watkins, R. W.; Arif, A.. M.; Berreau, L. M. *Inorg. Chem.* **2007**, *46*, 2353. (b) Ingle, G. K.; Watkins, R. W.; Arif, A. M.; Berreau, L. M. *J. Coord. Chem.* **2008**, *61*, 61.
(19) Hutchby, M.; Houlden, C. E.; Haddow, M. F.; Tyler, S. N. G.; Lloyd-Jones, G. C.; Booker-Milburn, K. I. *Angew. Chem., Int. Ed.* **2012**, *51*, 548.
(20) (a) Edwards, D. R.; Garrett, G. E.; Neverov, A. A.; Brown, R. S. *J. Am. Chem. Soc.* **2009**, *131*, 13738. (b) Liu, C. T.; Neverov, A. A.; Maxwell, C. I.; Brown, R. S. *J. Am. Chem. Soc.* **2010**, *132*, 35. (c) Raycroft, M. A. R.; Liu, C. T.; Brown, R. S. *Inorg. Chem.* **2012**, *51*, 3846.
(21) Sundberg, R. J.; Martin, R. B. *Chem. Rev.* **1974**, *74*, 471.
(22) For the designation of pH in non-aqueous solvents we use the nomenclature recommended by the IUPAC, *Compendium of Analytical Nomenclature. Definitive Rules 1997*, 3rd ed.; Blackwell: Oxford, U. K., 1998. The pH meter reading for an aqueous solution determined with an electrode calibrated with aqueous buffers is designated as ${}^{w}_{w}$pH; if the electrode is calibrated in water and the "pH" of the neat buffered methanol solution then measured, the term ${}^{s}_{w}$pH is used; and if the electrode is calibrated in the same solvent and the "pH" reading is made, then the term ${}^{s}_{s}$pH is used. In methanol ${}^{s}_{w}$pH-(−2.24) = ${}^{s}_{s}$pH and since the autoprotolysis constant of methanol is $10^{-16.77}$, neutral ${}^{s}_{s}$pH is 8.4. ${}^{s}_{s}pH_a$ refers to the negative log of the acid dissociation constant for the process **4**:Cu(II):$(HOCH_3)$ ⇌ **4**:Cu(II):$(^-OCH_3)$ measured in, and referenced to, solvent methanol.
(23) (a) Becke, A. D. *Phys. Rev. A.* **1988**, *38*, 3098. (b) Lee, C.; Yang, W.; Parr, R. G. *Phys. Rev. B.* **1988**, *37*, 785.
(24) (a) Tomasi, J.; Mennuccia, B.; Cancés, E. *THEOCHEM.* **1999**, *464*, 211. (b) Tomasi, J.; Mennuccia, B.; Cammi, R. *Chem. Rev.* **2005**, *105*, 2999.
(25) Frisch, M. J.; et al. *Gaussian 09*, Revision C.01; Gaussian, Inc.: Wallingford, CT, 2009.
(26) (a) Hay, P. J.; Wadt, W. R. *J. Chem. Phys.* **1985**, *82*, 270. (b) Wadt, W. R.; Hay, P. J. *J. Chem. Phys.* **1985**, *82*, 284.
(27) (a) Meresaar, U.; Bratt, L. *Acta Chem. Scand. A* **1974**, *28*, 715. (b) Bunton, C. A.; Nayak, B.; O'Connor, C. *J. Org. Chem.* **1968**, *33*, 572. (c) Meloche, I.; Laidler, K. J. *J. Am. Chem. Soc.* **1951**, *73*, 1712. (d) Broxton, T. J.; Deady, L. W.; Pang, Y.-T. *J. Am. Chem. Soc.* **1977**, *99*, 2268. (e) Slebocka-Tilk, H.; Bennet, A. J.; Keillor, J. W.; Brown, R. S.; Guthrie, J. P.; Jodhan, A. *J. Am. Chem. Soc.* **1990**, *112*, 8507. (f) Slebocka-Tilk, H.; Bennet, A. J.; Hogg, H. J.; Brown, R. S. *J. Am. Chem. Soc.* **1991**, *113*, 1288.
(28) (a) De Wolfe, R. H.; Newcomb, R. S. *J. Org. Chem.* **1971**, *36*, 3870. (b) Bender, M. L.; Thomas, R. J. *J. Am. Chem. Soc.* **1961**, *83*, 4183. (c) Kotch, A.; Krol, L. H.; Verkade, P. E.; Wepster, B. M. *Rec. Trav. Chim. Pays-Bas* **1952**, *71*, 108. (d) Biekart, H. J. B.; Dessens, H. B.; Verkade, P. E.; Wepster, B. M. *Rec. Trav. Chim. Pays-Bas* **1952**, *71*, 1246.
(29) (a) Schowen., R. L.; Hopper, C. R.; Bazikian, C. M. *J. Am. Chem. Soc.* **1972**, *94*, 3095. (b) Broxton, T. J.; Deady, L. W. *J. Org. Chem.* **1967**, *31*, 2767. (c) Broxton, T. J.; Deady, L. W.; Rowe, J. E. *J. Org. Chem.* **1980**, *45*, 2404. (d) Broxton, T. J.; Duddy, N. W. *Aust. J. Chem.* **1980**, *33*, 903. (e) Venkatasubban, K. S.; Schowen, R. L. *J. Org. Chem.* **1984**, *49*, 653. (f) Broxton, T. J.; Deady, L. W.; Rowe, J. E. *J. Org. Chem.* **1974**, *39*, 2767.
(30) Bennet, A. J.; Brown, R. S. Physical Organic Chemistry of Acyl Transfer Reactions. In *Comprehensive Biological Catalysis: A Mechanistic Reference*; Sinnott, M., Ed.; Academic Press: New York, 1997; Vol. *1*, pp 293−326.
(31) (a) Kershner, L. D.; Schowen, R. L. *J. Am. Chem. Soc.* **1971**, *93*, 2014. (b) Drake, D.; Schowen, R. L.; Jayaraman, H. *Ibid.* **1974**, *95*, 454.
(32) The methoxide promoted reaction of 0.15 M **4b** in 0.3 M $KOCH_3$ shows no indication of product formation after 52.5 days. Assuming we could detect 1 mM of the product, an upper limit for the second order rate constant is $k_{MeO^-} = 4.9 \times 10^{-9}$ M^{-1} s^{-1}. The rate law for reaction of the Cu(II) complex of **4b** as a function of ${}^{s}_{s}$pH is given as $k_{obs}^{4b} = k_x^{4b}\cdot({}^{s}_{s}K_a/({}^{s}_{s}K_a + [H^+]))$[12]. Under conditions where ${}^{s}_{s}K_a < [H^+]$, the reaction is first order in $[^-OCH_3]$. Given a ${}^{s}_{s}pK_a$ of 6.5[12] for formation of **4b**:Cu(II):$(^-OCH_3)(HOCH_3)$, and an autoprotolysis constant for methanol of $K_{auto} = 10^{-16.77}$ M^2, one computes that $k_{obs}^{4b} = k_x^{4b}\cdot({}^{s}_{s}K_a/(K_{auto}))[^-OCH_3]$. The apparent second order rate constant for the reaction of methoxide with **4b**:Cu(II):$(HOCH_3)_2$ is 5.3×10^{-3} $s^{-1}\cdot 10^{10.27}$ $M^{-1} = 10^8$ M^{-1} s^{-1}. This value is 2.0×10^{16} larger than the k_{MeO^-} for attack of methoxide on **4b** in the absence of the Cu(II).
(33) (a) Tommila, E.; Hinshelwood, C. N. *J. Chem. Soc.* **1948**, 1801. (b) Jaffé, H. H. *Chem. Rev.* **1954**, *53*, 192.
(34) It is a valid comment that "..... a (partial) positive charge should be present on this N and the conjugation of the electron pair with the C═O should be less important than in a regular amide. Compared to a "normal" amide bond this one is ... higher in energy and, consequently, closer in energy to the transition state for methanolysis." We thank the referee for the opportunity to discuss this point within the context of destabilization of a substrate through binding to a catalyst.
(35) For a discussion of the hydrolysis and reactivity of acylammonium species in water see: Williams, A. *J. Am. Chem. Soc.* **1976**, *98*, 5645.
(36) For a discussion of the decrease of the rotational barrier of amides **1** and **4** in the presence of Cu(II) and other metals see: (a) Cox, C.; Ferraris, D.; Murthy, N. N.; Lectka, T. *J. Am. Chem. Soc.* **1996**, *118*, 5332. (b) Cox, C.; Lectka, T. *Acc. Chem. Res.* **2000**, *33*, 849.
(37) The DFT-computed transition state free energies for interconverting the planar and orthogonal forms of the amides by rotation about the amidic N-C═O(R) bond in a methanol continuum are 22.1and 20.8 kcal/mol for **4b** and **1** respectively, and 18.7 and 15.9 kcal/mol for their respective Cu(II):$(^-OMe)(HOMe)$ complexes. See Supporting Information.
(38) (a) Jencks, W. P. *Adv. Enzymol.* **1975**, *43*, 219. (b) Jencks, W. P. *Adv. Enzymol.* **1980**, *51*, 75. (c) Bruice, T. C. *The Enzymes*; Boyer, P. D., Ed.; Academic Press: New York, 1970; Vol. *11*, pp 217−279. (d) Fersht, A. *Enzyme Structure and Mechanism*; 2nd ed.; W. H. Freeman: San Francisco, 1985; pp 311−346. (e) Jencks, W. P. *Catalysis in Chemistry and Enzymology*; McGraw-Hill: New York, 1969. (f) Wolfenden, R. *Acc. Chem. Res.* **1972**, *5*, 10. (g) Haldane, J. B. S. *Enzymes*; Longmans, Green and Co.: London, U.K., 1930; (h) Lumry, R. *The Enzymes*; Boyer, P. D., Ed.; Academic: New York, 1959; Vol. *I*, pp 157−258.
(39) (a) Pauling, L. *Nature* **1948**, *161*, 707. (b) Pauling, L. *Am. Sci.* **1948**, *36*, 51.
(40) Zhang, X.; Houk, K. N. *Acc. Chem. Res.* **2005**, *38*, 379.
(41) (a) Liu, C. T.; Maxwell, C. I.; Edwards, D. R.; Neverov, A. A.; Mosey, N. J.; Brown, R. S. *J. Am. Chem. Soc.* **2010**, *132*, 16599. (b) Liu, C. T.; Neverov, A. A.; Brown, R. S. *Inorg. Chem.* **2011**, *50*, 7852.
(42) Liu, C. T.; Maxwell, C. I.; Pipe, S. G.; Neverov, A. A.; Mosey, N. J.; Brown, R. S. *J. Am. Chem. Soc.* **2011**, *133*, 20068.
(43) Gibson, G.; Neverov, A. A.; Brown, R. S. *Can. J. Chem.* **2004**, *81*, 495.
(44) Carvalho, N. M. F.; Horn, A., Jr.; Bortoluzzi, A. J.; Drago, V.; Antunes, O. A. C. *Inorg. Chim. Acta* **2006**, *359*, 90.